analytical chemistry

Article

Cite This: Anal. Chem. 2019, 91, 2360−2367

pubs.acs.org/ac

Femtomolar Detection of Lipopolysaccharide in Injectables and Serum Samples Using Aptamer-Coupled Reduced Graphene Oxide in a Continuous Injection-Electrostacking Biochip

Junxin Niu,[†] Xiumei Hu,[‡] Wei Ouyang,[§] Yue Chen,[†] Shuwen Liu,[†] Jongyoon Han,*[,§,∥] and Lihong Liu*[,†]

[†]Guangdong Provincial Key Laboratory of New Drug Screening, School of Pharmaceutical Sciences, Southern Medical University, Guangzhou 510515, China

[‡]Department of Laboratory Medicine, Nanfang Hospital, Southern Medical University, Guangzhou 510515, China

[§]Department of Electrical Engineering and Computer Science, Massachusetts Institute of Technology, Cambridge, Massachusetts 02139, United States

[∥]Department of Biological Engineering, Massachusetts Institute of Technology, Cambridge, Massachusetts 02139, United States

Supporting Information

ABSTRACT: A method for microfluidic sample preconcentration to detect femtomolar level of lipopolysaccharide (LPS) is introduced, enabled by 6-carboxyfluorescein (6-FAM) labeled aptamer-LPS binding along with reduced graphene oxide (rGO). The free FAM-aptamers can be adsorbed onto the surface of rGO, resulting in fluorescence quenching of background signals. Conversely, the aptamer−LPS complex cannot be adsorbed by rGO, so the fluorescence is maintained and detected. When an electric field is applied across the microchannel with Nafion membrane in the chip, only the fluorescence of aptamer−LPS complex can be detected and stacked by continuous injection-electrostacking (CI-ES). The method shows a high selectivity (in the presence of pyrophosphate, FAD^+, NAD^+, AMP, ADP, ATP, phosphatidylcholine, LTA, and β-D-glucans which respond positively to LAL) to LPS and an extreme sensitivity with the limit of detection (LOD) at 7.9 fM (7.9×10^{-4} EU/mL) and 8.3 fM (8.3×10^{-4} EU/mL) for water sample and serum sample, respectively. As a practical application, this method can detect LPS in injections and serum samples of human and sepsis model mouse and quickly distinguish Gram-negative bacteria *Escherichia coli* (*E. coli*) from Gram-positive bacteria *Staphylococcus aureus* (*S. aureus*) and fungus *Candida albicans* (*C. albicans*). More importantly, by changing the aptamers based on different targets, we can detect different analytes. Therefore, aptamer-coupled rGO in a CI-ES biochip is a universal, sensitive, and specific method. For TOC only

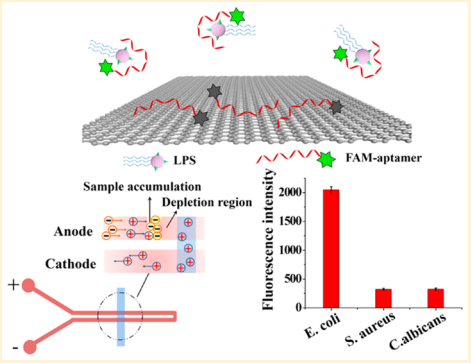

Lipopolysaccharide (LPS), also known as endotoxin, is a characteristic component in the outer membrane of Gram-negative bacteria.[1] LPS is released upon the death of bacterial cells. LPS is a highly toxic inflammatory stimulator and can lead to fever, sepsis or septic shock, multi-organ failure, and even death,[2] causing about 700000 cases of patients with severe medical problems and 250000 cases of casualties annually in the United States.[3] The main reason is that immune cells (monocytes, macrophages, and dendritic cells) are the most sensitive responders of LPS. LPS can interact with the specialized cellular receptors, such as Toll-like receptor-4/MD2 and CD14, resulting in the production of inflammatory cytokines.[4] Because of the potential of severe immune responses, testing for LPS is a vital part of ensuring the safety of sterilized products, especially in the fields of biological products derived from Gram-negative bacteria, medical devices, parenteral drugs, food and water security, etc. The maximum allowable LPS levels in pharmaceutical products and medical devices are 5 EU/kg/h (50 fmol/kg/h) for most drug products and 0.2 EU/kg/h (2 fmol/kg/h) for intrathecally administered drugs.[5] Furthermore, due to its high toxicity even at low concentrations, 10 pg/mL (1 pM, 0.1 EU/mL) of LPS is the cutoff value to distinguish between healthy and Gram-negative bacteremia patients in clinical setting,[6] and typical LPS levels in patients with sepsis are 300 pg/mL (30 pM, 3 EU/mL).[7] These data clearly demonstrate the importance of highly sensitive and accurate detection of LPS.

Although the gold-standard method enzymatic limulus amebocyte lysate (LAL) assay for LPS detection is widely used in many fields,[8] it is highly susceptible to temperature, pH changes, and interference factors and requires tedious sample preparation procedures. More importantly, LAL preparation depends on limulus (horseshoe crab), the number of which has

Received: November 5, 2018
Accepted: December 21, 2018
Published: December 21, 2018

DOI: 10.1021/acs.analchem.8b05106
Anal. Chem. 2019, 91, 2360−2367

seriously decreased because of overfishing. Therefore, it is an urgent need to develop an alternative for the LAL test. In recent years, diverse methods for LPS detection have been developed. However, traditional alternative methods such as the Western blot, mass spectrometry, and gel electrophoresis do not reach sensitivities equivalent to that of the LAL test.[9,10] Currently, electrochemical and optical sensors based on anti-LPS antibodies, peptides, or aptamers possess considerable promises to overcome the weaknesses of traditional methods,[11,12] but the practical application of antibody-based biosensors is still limited by their high costs, long turn-around time, and labor intensiveness. Furthermore, it is still a great challenge to detect LPS at the femtomolar level. There is a pressing need for new methods to reliably detect LPS in serum samples at toxic concentrations.

Aptamers are essentially short single-stranded oligonucleotides (RNA or DNA), which function as high-specificity and high-affinity ligands. In principle, aptamers can bind to any given target molecules in vitro by folding into unique three-dimensional structures, ranging from small molecules to large proteins and even cells.[13] Recently, biosensors based on LPS-recognizing aptamers have been developed,[14,15] but the skill-intensiveness and high cost limit their application.

Graphene oxide (GO) is a two-dimensional (2D) carbon crystal and has attracted great attention because of its excellent thermal and chemical stability and high surface area.[16] rGO possesses better water dispersibility and a prominent fluorescence quenching effect because of the presence of more crystalline graphene regions on the sheets compared with GO.[17] Fluorescence-labeled aptamer (ssDNA) can be adsorbed well and efficiently quenched by the rGO surface because of the hydrophobic and $\pi-\pi$ stacking interactions between the rings of nucleobases and the hexagonal surfaces of the rGO.[18] This remarkable property has been used for the detection of various targets based on differences in the degree of fluorescence quenching. However, the biocompatibility of graphene is very low,[19] which will affect the biorecognition process. Most importantly, the selectivity and sensitivity of graphene-based sensors are restricted.

Microfluidic chips are miniaturized and integrated biochips using common buffer solutions and reagents. Additionally, many stacking methods have been developed on microfluidic chips that are easy to be combined with various detectors,[20,21] and various continuous injection concentrators bring promises to point-of-care tests in personalized assays. Continuous injection-electrostacking (CI-ES) devices based on an ion-selective membrane can continuously collect negatively charged analytes, thereby achieving highly sensitive and quantitative determination of low-abundance biomolecules. In a word, biochip is a promising choice to address many deficiencies of conventional biosensing techniques.

Given all of that, we present a new method of LPS detection based on CI-ES in a polydimethylsiloxane (PDMS) chip under a DC electric field using FAM and rGO as the fluorescence signal reporter and quencher, respectively. Our results indicate that this system is capable of determining LPS with very high sensitivity in various practical samples with less time (30 min) and simpler experimental setup.

EXPERIMENTAL SECTION

Reagents and Chemicals. Tris-base, boric acid, and ethylenediamine tetraacetic acid disodium salt were supplied by Biosharp, Tianjin Fuchen Chemical Reagents Factory, and Guangzhou Jinhuada Chemical Reagents Co., Ltd., respectively. Trichlorosilane and platinum wire electrode were supplied by Macklin (Shanghai, China) and Xiya Reagents (Shandong, China), respectively. Then 20 wt % Nafion resin, NAD^+, FAD^+, phosphatidylcholine, lipoteichoic acid from *Staphylococcus aureus*, β-D-glucans from barley, and LPS from *Escherichia coli* 055:B5 were purchased from Sigma-Aldrich (USA). The molecular weight of LPS was assumed to be 10 kDa in our work.[12,22,23] AMP, ADP, ATP, and pyrophosphate were purchased from Stanford (Eugene, Oregon, USA). Graphene oxide (GO) was purchased from Suzhou Hengqiu Graphene Technology Co., Ltd. FAM-labeled aptamer is an 86-base oligonucleotide (5′-CTTCTGCCCGCCTCCTTC-CTAGCCGGATCGCGCTGGCCAGATGATATA-AAGGGTCAGCCCCCCAGGAGACGAGATAGG-CGGACACT-3′, K_d value of 12 nM), which was synthesized by Guangzhou IGE Biotechnology Ltd. The elastomer used in this work is General Electric Silicones RTV 615. The RTV 615 base and curing agent were mixed at a 10:1 ratio by weight. *E. coli* ATCC 25922 and *S. aureus* ATCC 25923 were obtained from Guangdong Culture Collection Center. *Candida albicans* was obtained from clinical isolates of Nanfang Hospital (Gugngzhou, China), and the pyrogen-free pipet tips and Eppendorf tubes in all performed experiments were purchased from Axygen (MA, USA).

Apparatus. DC voltages were applied by a DC power supply (MP3001D, Maisheng, Dongguan, China). Fluorescence images were acquired using an inverted fluorescence microscope (Leica DMIL LED) equipped with a CCD camera (Leica DFC 360 FX) and analyzed using the ImageJ software. LPS widely exists in nature, thus all samples preparation was performed in a Class I biosafety cabinet. Ultrapure water was prepared by the Millipore Milli-Q water purification system (18.2 MΩ·cm, Millipore). The characteristics of GO and rGO were determined via scanning electron microscopy (SEM) (JSM-7001F, Japan), a Nanodrop 2000C (Thermo Scientific, Waltham, USA), and a Malvern Zetasizer Nano ZS instrument (Malvern, US).

Sample Preparation. The sample pretreatment processes were as follows: 6-carboxyfluorescein-labeled aptamer (FAM-aptamer, 6 nM) was first heated at 95 °C for 10 min and then immediately cooled at 15 °C for 10 min. Then the FAM-aptamer and LPS samples with water matrix were mixed and incubated at 15 °C for 10 min; Finally, rGO (15 μg/mL for serum samples and 10 μg/mL for water samples) and 1× TBE buffer were added into the mixture for a total volume of 200 μL and incubated at room temperature for 30 min on a rotary mixer. The serum matrix was prepared as follows: blood sample was first collected from healthy individual, then blood was centrifuged at 300*g* for 5 min to remove cellular components; next, 20 μL (the minimum serum volume is 1 μL, 20 μL was chosen to decrease measuring error) of serum samples were spiked with various concentration LPS standard solutions and mixed with β-mercaptoethanol (5% v/v) and SDS (10 mg/mL) in an Eppendorf tube, and 1× TBE buffer was added to a final volume of 200 μL; finally, the mixture was boiled for 5 min. Other processes are the same as those for the water matrix. The serum was diluted by 100 times to decrease the interference of sample matrix.

Microchip Fabrication. The silicon mold was fabricated following standard microfabrication processes: the desired pattern was constructed by photolithography onto a silicon wafer, followed by a deep reactive ion etching (DRIE) process

DOI: 10.1021/acs.analchem.8b05106
Anal. Chem. 2019, 91, 2360−2367

with an etching depth of 10 μm. The silicon mold was incubated overnight with trichlorosilane in a vacuum desiccator to prevent PDMS adhesion to the mold. The microchannel was fabricated by the standard PDMS molding technique. The Nafion membrane was patterned on a glass slide using the microflow patterning technique. A 45 μm thick and 400 μm wide microchannel with two punched holes was used as the flow channel for the Nafion resin. Then 1 μL of Nafion resin was loaded into the inlet of the straight channel. The Nafion resin can flow along the microchannel automatically because of capillary force and self-stopped at the outlet. The Nafion resin was cured by heating at 95 °C on the hot plate for 5 min. Finally, the PDMS chip was irreversibly bonded to the Nafion-patterned glass slide by plasma bonding. The Nafion membrane dimension can be controlled by varying the channel dimension of the silicon microchannel. Nafion is patterned perpendicularly to the concentration channel. Then 1−10 μL pipet tips were inserted into the punched holes as reservoirs.

Microfluidic Experiments. Before the experiment, the microchannel was passivated with 1% bovine serum albumin (BSA) for 10 min at room temperature to prevent nonspecific adhesion such as adsorption of LPS and the complex of aptamer−LPS to the microchannel surface. The channel was washed with ultrapure water three times and filled with 1× TBE buffer before loading the samples. All assays were performed using 1× TBE (pH 7.4) buffer. Platinum electrodes were inserted into the reservoirs and connected to a DC power supply. DC voltages were applied in all experiments (30 V for the samples with water matrix and 20 V for the samples with serum matrix). Fluorescence images were acquired with an exposure time of 300 ms. A mechanical shutter was used to reduce the photobleaching effect, which was synchronized with the CCD camera by the open source software Micromanager.

Preparation of rGO. It has been reported that rGO has better characteristics of quenching free fluorescence DNA than GO.[24] rGO was prepared by the hydrothermal reduction method.[25] The specific steps were as follows: A total of 50 mL of 0.05 mg/mL GO aqueous solution was added to a Teflon-lined autoclave and then heated at 180 °C for 6 h, followed by cooling to room temperature. The characterization of GO and rGO is shown in Supporting Information, Figures S1−S4.

Bacteria Sample Preparation. Fresh *E. coli*, *S. aureus*, and *C. albicans* were diluted in 1× TBE buffer solution (pH 7.4) for detection. The bacteria were collected by centrifugation at 4000 rpm for 10 min and rinsed with 1× TBE (pH 7.4), then broken by centrifugation at 13000 rpm for 10 min, and were finally resuspended in 1× TBE solution.

Experimental Mouse Model of Sepsis. The 6−7-week-old specific-pathogen-free (SPF) KM mice used in our study were obtained from the Experimental Animal Center of Southern Medical University (Guangzhou, China). Their weight on the day of the experiment was 29.2 ± 0.8 g. All the experiments were performed in line with the National Guide for the Care and Use of Laboratory Animals. In the animal experiments, 15 mg/kg body weight of LPS was injected intraperitoneally. Then 0.3 mL of blood was collected from each mouse for the LPS test at 4 and 12 h after the injection of LPS, respectively. The anal temperature of the mice decreased from 37.1 to 32.5 °C after LPS injection.[26] Serum samples were separated by centrifugation from the blood samples at 300*g* for 10 min.

Data Analysis. Fluorescence images were analyzed by the software ImageJ. Background blank value was subtracted from the image using the Subtract function of ImageJ. Next, the concentration fluorescence bands near the Nafion was measured (Image → Adjust → Threshold) to obtain fluorescence intensity.

RESULTS AND DISCUSSION

The Mechanism of Preferential Adsorption of rGO. Fluorescently labeled ssDNA aptamers can be adsorbed rapidly by the hydrophobic and $\pi-\pi$ stacking interactions at room temperature, which results in fluorescence quenching of the dye by fluorescence resonance energy transfer (FRET).[18] However, the aptamer−LPS complex has weak affinity to rGO, thereby retaining the fluorescence of the dye (Figure 1a). To characterize this mechanism, the zeta-potential analysis was carried out in 1× TBE buffer solution (pH 7.4), which was consistent with sample matrix in our experiments. The zeta-potentials of rGO (10 μg/mL) and FAM-aptamer (6 nM) were −28.4 and −5.05 mV, respectively, indicating FAM-aptamer is less negatively charged. However, the zeta-potential of the complex of FAM-aptamer−LPS was increased to −16.1 mV. It is because LPS has a high zeta-potential of −17.8 mV at 1 nM. On the basis of these results, it is reasonable to conclude that the negatively charged complex did not combine with rGO due to the electrostatic repulsion.

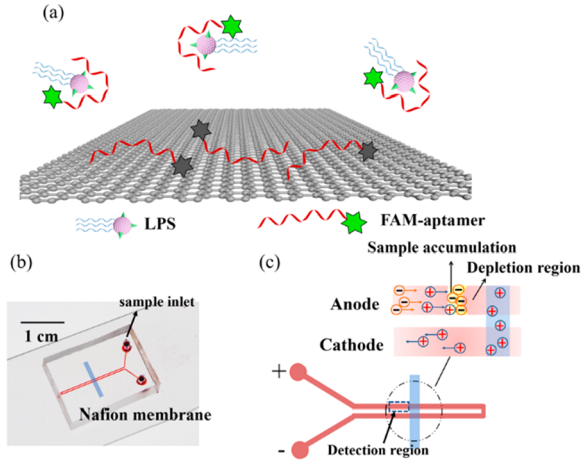

Figure 1. Mechanism of determination of LPS by coupling FAM-aptamer and rGO based on the CI-ES method using a microfluidic biochip. (a) Schematic representation of the fluorescence generation of LPS. (b) Schematic diagram of the PDMS microfluidic CI-ES-chip. The chip includes a Y shaped channel and a Nafion membrane. (c) Voltage scheme used for the LPS preconcentration and the CI-ES mechanism.

The Mechanism of CI-ES Method Coupling FAM-Aptamer of LPS and rGO. The optical image of the actual CI-ES-chip used in the experiments is shown in Figure 1b. The Nafion membrane, which is composed of nanometer-sized ion-selective pathways, has strong cation selectivity and higher conductivity compared to that of the buffer solution in a microchannel.[27] Therefore, it is often used as an ion-permselective nanoporous membrane in microfluidic preconcentration devices.[28] When an electric field is applied across the microchannel with Nafion membrane in the device, an ion depletion zone is created in the channel at the vicinity of the Nafion membrane due to the concentration polarization

DOI: 10.1021/acs.analchem.8b05106
Anal. Chem. 2019, 91, 2360−2367

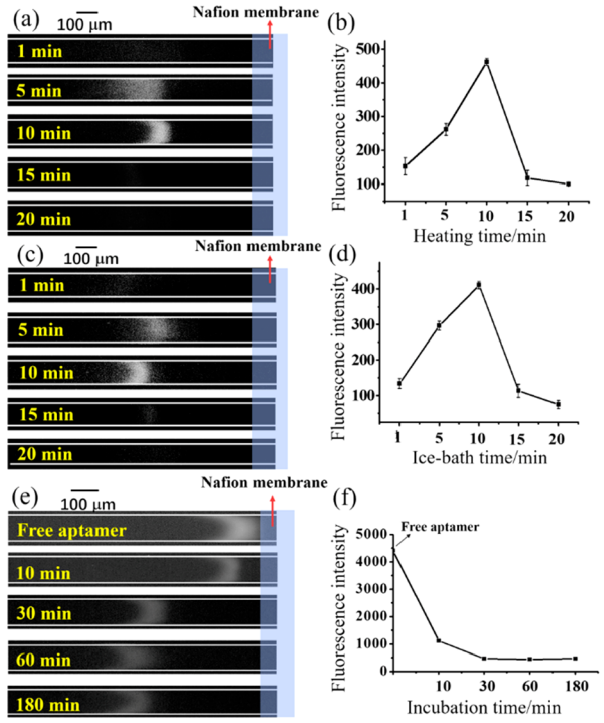

Figure 2. (a) Effect of heating time of aptamer on concentrated fluorescence band. (b) Effect of heating time on sample accumulation. (c) Effect of ice-bath time of aptamer on concentrated fluorescence band. (d) Effect of ice-bath time on sample accumulation. (e) Effect of incubation time of rGO on concentrated fluorescence band, and the first fluorescence band was produced by the free aptamer sample without LPS and rGO. (f) Effect of incubation time on sample accumulation. Conditions: 1× TBE (pH 7.4, 25% v/v CH_3OH). Nafion microchannel dimension: 400 μm width and 45 μm depth; rGO 10 μg/mL, 30 V; LPS concentration is 1 pM (0.1 EU/mL), sample matrix is water.

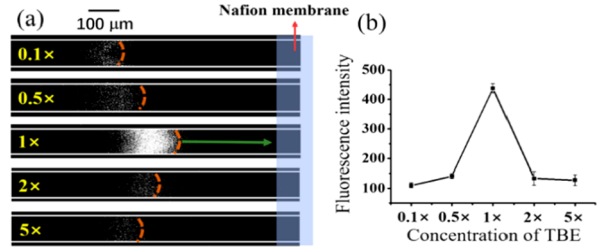

Figure 3. (a) Effect of TBE concentration on enrichment fluorescence. (b) Dependence of enrichment fluorescence intensity on TBE concentration. Aptamer heating and ice-bath time both were 10 min, and incubation time with rGO was 30 min, other conditions as in Figure 2.

phenomena.[29] According to the classic theory of ion concentration polarization (ICP), the ion depletion zone was developed based on a force balance between electrophoresis and electroosmotic flow.[21,30] As shown in Figure 1c, when DC voltage is applied across the microchannel, the electric field is significantly amplified near the Nafion membrane due to the ion depletion. The negatively charged aptamer−LPS complex is subject to two counteracting effects: it is repelled from the depletion zone by the electrostatic force and, at the same time, moved toward the depletion zone by an electroosmotic flow (EOF) produced by an electric field, which leads to the continuous accumulation of the aptamer−LPS complex where

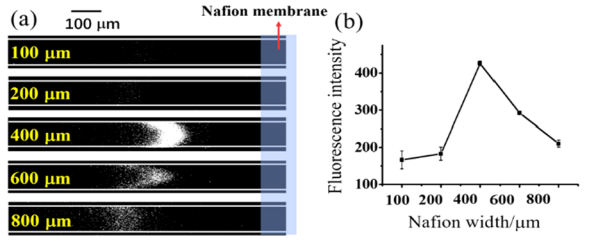

Figure 4. (a) Effect of Nafion microchannel width on concentrated fluorescence band. (b) Dependence of enrichment fluorescence intensity on Nafion microchannel width. Conditions: 1× TBE (pH 7.4), 25% v/v CH_3OH, other conditions as in Figure 3.

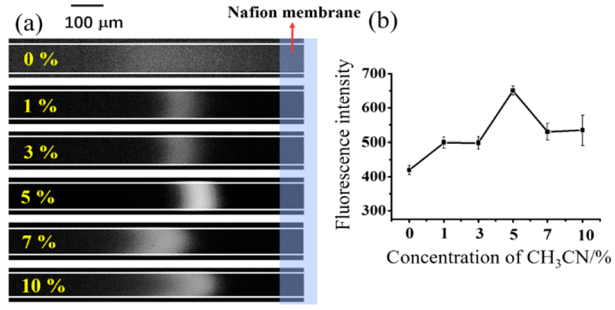

Figure 5. (a) Effect of CH_3CN concentration on serum sample accumulation. (b) Dependence of enrichment fluorescence intensity on concentration of CH_3CN. The sample matrix is serum, rGO 15 μg/mL, 20 V, other conditions as in Figure 3.

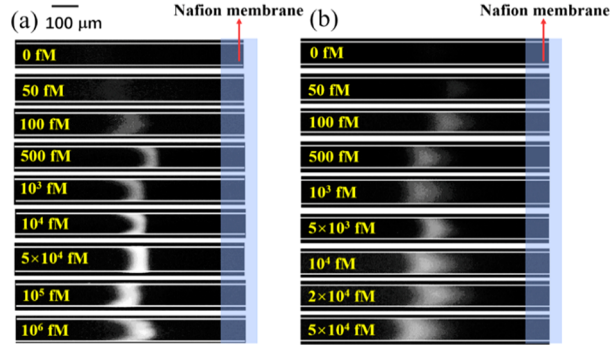

Figure 6. CI-ES-chip for detecting LPS in (a) water sample and (b) 1% serum sample after 30 min of concentration.

Table 1. Regression Equations, Correlation Coefficients (r), Linear Ranges, LODs, and RSDs for CI-ES Chip

sample	water sample	serum sample
regression equation[a]	$y = 117.88\ln(x) - 336.06$	$y = 139.58\ln(x) - 397.93$
r	0.9977	0.9952
linear range (fM)	$50 - 10^6$	$50 - 5 \times 10^4$
LOD(S/N = 3) (fM)	7.9 fM (7.9×10^{-4}EU/mL)	8.3 fM (8.3×10^{-4}EU/mL)
RSD (%)	2.5	3.2

[a] $y = a\ln(x) + b$; y, fluorescence intensity; x, standard concentration (fM).

electrophoresis and electroosmosis balance, near the anodic edge of the Nafion membrane. In short, CI-ES can concentrate aptamer−LPS complex by the nanojunction-induced ion depletion effect in a microchannel. The fluorescence intensity is correlated to the concentration of LPS, which can imply the quantity of LPS in the samples.

DOI: 10.1021/acs.analchem.8b05106
Anal. Chem. 2019, 91, 2360−2367

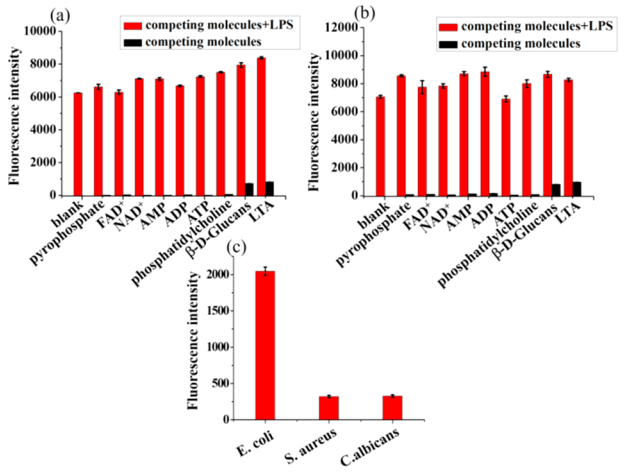

Figure 7. (a,b) Selectivity of the CI-ES-chip to LPS in water and serum matrix, respectively. It is shown that fluorescence intensity upon the addition of some competing biological molecules and LPS (upon the addition of 1 μM competing biological molecules and further addition of 1 μM LPS in samples). Blank represents only LPS in sample solution. Red and black bars represent the competing molecules in the presence and absence of LPS, respectively. (c) Fluorescence intensity of three kinds of bacteria (10^8 cfu/mL) after 30 min of CI-ES at 30 V.

The Optimization of Experimental Conditions. To achieve high-sensitivity and rapid detection, the optimizations of the buffer medium and reaction conditions are of primary importance. In addition, due to the complex matrix of serum, sample medium of serum is optimized solely.

Effect of the Incubation Time of Heating and Ice-Bath. On the basis of a prior study,[31] the aptamer was heated at 95 °C and then immediately cooled at 15 °C, which made it easier to form the secondary structure. The heating time and the ice-bath time were investigated from 1 to 20 min. Parts a and c of Figure 2 reveal that fluorescence response is enhanced and the fluorescence band is condensed with the heating time and ice-bath time increased up to 10 min. It is because that aptamer needs adequate time to form a stable structure that can line with LPS more completely. However, the fluorescence intensity and stability of the band decrease significantly beyond 10 min, as shown in Figure 2b,d. Therefore, 10 min is chosen as the optimum for heating and ice-bath time.

Effect of the Incubation Time of rGO. To determine how the incubation time (15 °C) of rGO in the mixture of free aptamer and aptamer−LPS complex affected sensitivity, a more exhaustive study was performed. The incubation time was optimized in the range from 30 to 180 min. Parts e and f of Figure 2 reveal that the fluorescence intensity of the mixture decreased up to 30 min and then remained constant with increased the incubation time, suggesting that free aptamer is adsorbed completely. Therefore, 30 min was chosen.

Effect of TBE Concentration. Buffer concentration has a direct influence on the EOF and the viscosity of the buffer. The effect of the TBE concentration from 0.1× to 5× was investigated. The distance from the Nafion membrane (anodic side) to the depletion boundary (brown dotted line) is defined as the depletion length (green arrow). Figure 3a illustrates the behavior of the sample stacking and depletion lengths under different TBE concentrations after 30 min of CI-ES at 30 V. As expected, the fluorescence intensity increases with the TBE concentration up to 1× but decreased at 2× and 5× (Figure 3b), and the depletion distance in lower concentrations is longer than that in higher concentration buffer because in lower concentrations, the negatively charged analyte moves toward the anode in order to maintain electroneutrality; however, in higher concentrations, with cations in the channel, it is not necessary for the negatively charged analytes to move further toward the anode to maintain the electroneutrality.[16] The shorter depletion length (due to higher conductivity gradient lead to higher electric field gradient) resulted in the better stacking efficiency. In the case of 2× or 5× TBE, the large amount of ions affected the accumulation efficiency due to the collapse of the ion depletion zone, resulting in decreased fluorescence. So as to obtain a stable concentrated strip, 1× TBE is chosen.

Effect of Nafion Width. We investigated the effect of Nafion width on the accumulation efficiency. As shown in Figure 4a, there is less stacking when the Nafion width is less than 200 μm. The reason is that the conductance through the Nafion membrane is lower than that of the channel, which results in the loss of samples through the ion depletion zone.[20] Our results indicate that the fluorescence intensity of LPS increased with the width of the Nafion membrane up to 400 μm and then decreased at higher widths of the Nafion membrane (Figure 4b). Wider Nafion membranes up to 400 μm result in better stacking efficiency due to the increase of electric field gradient (the increase in conductivity gradient).[20] However, oversized Nafion would lead to stronger ICP, leading to longer depletion lengths and therefore reduced field gradients traps for trapping the molecules.

Effect of CH_3CN Concentration in Buffer. In this study, the concentrations of CH_3CN were studied from 0% to 10%. The addition of CH_3CN in the TBE buffer was found to improve the stability and compactness of band shape. Figure 5a presents that the fluorescence band of the serum sample is loose without CH_3CN as a modifier. CH_3CN provide a higher electric field, which enabled the analytes to be focused sharply.[32] It was also observed that the fluorescence sensitivity initially improved with addition of CH_3CN up to 5% and gradually decreased with the further addition of CH_3CN (Figure 5b). CH_3CN stacking is known as an online sample preconcentration method. The narrowing of the fluorescence band can be explained by the mechanism of transient "pseudo-ITP".[32] However, it also increases the mismatch of electro-osmotic velocities between sample solution and buffer, which results in laminar flows and broadening of the stacked zone.[33] Therefore, a proper compromise should be made to get the best results, and 5% v/v CH_3CN was chosen for further studies.

The final optimized conditions are as follows. (1) Water matrix: aptamer heating and ice-bath time are 10 min, and incubation time with rGO is 30 min; the Nafion microchannel dimension is 400 μm width and 45 μm depth; the buffer concentration is 1 × TBE (pH 7.4), 25% v/v CH_3OH); the rGO concentration is 10 μg/mL; the DC voltage is 30 V. (2) Serum matrix: aptamer heating and ice-bath time are 10 min, and incubation time with rGO is 30 min; Nafion microchannel dimension is 400 μm width and 45 μm depth; the buffer concentration is 1× TBE (pH 7.4), 25% v/v CH_3OH, 5% v/v CH_3CN; the rGO concentration is 15 μg/mL; the DC voltage is 20 V. Other condition optimizations are presented in the Supporting Information.

Method Validation. The linearity was measured by plotting the fluorescence intensity (y) of LPS versus the

DOI: 10.1021/acs.analchem.8b05106
Anal. Chem. 2019, 91, 2360−2367

Table 2. Results for Determination of LPS in Real Samples (n = 10)

sample	ingredient	content/pM (EU/mL)	spiked/pM (EU/mL)	found/pM (EU/mL)	recovery (%)	average (%)	RSD (%)	LAL test/pM (EU/mL)
serum of healthy mouse	LPS	0.92 (0.092)	0.4 (0.04)	1.26 (0.126)	80	85	3.3	0.85 (0.085)
			0.8 (0.08)	1.57 (0.157)	88		6.2	
			1.2 (0.12)	1.95 (0.195)	85		4.1	
serum of sepsis model mouse (4 h)	LPS	30.1 (3.01)	20 (2.0)	47.56 (4.756)	89	89	3.4	36.0 (3.60)
			40 (4.0)	63.28 (6.328)	91		5.5	
			60 (6.0)	80.38 (8.038)	86		1.0	
serum of sepsis model mouse (12 h)	LPS	30.4 (3.04)	20 (2.0)	48.44 (4.844)	86	84	3.3	35.7 (3.57)
			40 (4.0)	65.44 (6.544)	86		2.5	
			60 (6.0)	79.66 (7.966)	81		5.0	
water for injection (veterinary)	LPS	0.32 (0.032)	0.1 (0.01)	0.40 (0.04)	114	96	6.3	0.42 (0.042)
			0.3 (0.03)	0.53 (0.053)	81		8.6	
			0.6 (0.06)	0.86 (0.086)	95		9.1	
NaCl injection	LPS	[a]	1.0 (0.1)	0.87 (0.087)	87	85	5.9	
			5.0 (0.5)	4.12 (0.412)	82		7.2	
glucose injection	LPS		1.0 (0.1)	0.97 (0.097)	97	89	8.1	
			5.0 (0.5)	4.05 (0.405)	81		6.5	
water for injection	LPS		1.0 (0.1)	0.90 (0.09)	90	85	8.3	
			5.0 (0.5)	4.02 (0.402)	80		3.8	
tap water	LPS	9.2 (0.92)	5.0 (0.5)	13.39 (1.339)	84	94.6	5.1	9.80 (0.98)
			10.0 (1)	20.58 (2.058)	114		2.6	
			15.0 (1.5)	22.10 (2.21)	86		3.0	
zinc gluconate oral solution	LPS	0.3 (0.03)	0.1 (0.01)	0.39 (0.039)	87	84	2.9	0.22 (0.022)
			0.3 (0.03)	0.54 (0.054)	81		4.0	
			0.5 (0.05)	0.72 (0.072)	82		4.1	
calcium gluconate oral solution	LPS		0.3 (0.03)	0.25 (0.025)	85	90	4.0	
			0.5 (0.05)	0.47 (0.047)	95		1.7	

[a]No detection.

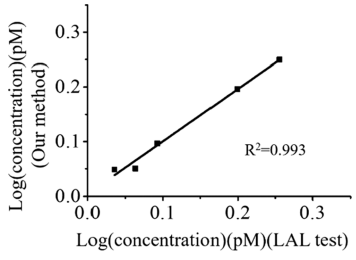

Figure 8. Benchmarking of our method with a commercial LAL kit from Xiamen Bioendo Technology. The current standard deviation for our method is <2.7. The coefficient of variation (CV) of the LAL test is <3.0%.

corresponding concentration (x). Calibration graphs were obtained by determining standard solutions of LPS at eight different concentrations (50, 100, 500, 10^3, 10^4, >5 × 10^4, 10^5, and 10^6 fM, and 50, 100, 500, 10^3, 5 × 10^4, 10^4, 2 × 10^4, and 5 × 10^4 fM for water and serum matrix, respectively). Figure 6 presents the results of detecting LPS in water and serum samples. Each point corresponds to the mean value of three independent fluorescence values. The RSD of the fluorescence for three replicate runs is <4.0%. The LOD (LOD = 3 × SD/k) is calculated to be 7.9 fM (7.9 × 10^{-4} EU/mL) and 8.3 fM (8.3 × 10^{-4} EU/mL) for the water sample and the serum sample, which is the lowest value reported thus far, and the sensitivity enhancement factor (SEF) of this device is 257. The corresponding regression equations, as well as other characteristic parameters for the determination of LPS, are listed in Table 1.

Selectivity of Coupling FAM-Aptamer with rGO Based on CI-ES Chip. Specificity plays a key role for the practical application of aptamer functionalization of the rGO sensor. The selectivity of the aptamer for LPS is evaluated by the fluorescence intensity response in the presence of various important competing biological molecules (pyrophosphate, FAD^+, NAD^+, AMP, ADP, ATP, phosphatidylcholine, LTA, and β-D-glucan) in the sample solution. As shown in Figure 7a,b, this method shows high target specificity. All of the other biological molecules did not give rise to significant increase in fluorescence intensity, even the addition of LTA and β-D-glucan. As we know, LTA and LPS have closely similar

DOI: 10.1021/acs.analchem.8b05106
Anal. Chem. 2019, 91, 2360−2367

molecular structures, both of which contain phosphates and long hydrophobic chains, and β-D-glucan can interfere with the detection of LPS with LAL test kits, but in our work, only LPS could induce remarkable change of the fluorescence intensity. A quantitative description of the degree of interference (DI)[34] for competing molecules is shown in Supporting Information, Table S1. The results reveal that the coupling FAM-aptamer with rGO based on the CI-ES-chip has high capacity of resisting disturbance to the biological competing molecules.

Discrimination of Gram-Negative Bacteria from Gram-Positive Bacteria and fungus. Bacterial contamination is a major health hazard in both foods and drugs. Sepsis caused by Gram-negative bacteria, Gram-positive bacteria, and fungus often manifest similar clinical features. Therefore, identifying the causative pathogen is critical for the successful antimicrobial treatment of sepsis. Microbiological examinations are the current gold standard to identify causative pathogens. However, bacteraemia is identified in only about 30% of patients with sepsis.[35] Therefore, it is urgent to develop sensitive and specific methods for discriminating Gram-negative sepsis from Gram-positive and fungal sepsis. Our method is highly specific and sensitive to LPS, thus possible to distinguish Gram-negative bacteria from Gram-positive bacteria and fungal. In this study, *E. coli* (Gram-negative bacteria), *S. aureus* (Gram-positive bacteria), and *C. albicans* (fungus) were used as example targets. Fresh bacterial suspensions ($C = 10^8$ cfu/mL) were used for our test under the optimum conditions obtained from the experiments described above. Figure 7c presents that the fluorescence values of three kinds of bacteria obtained by our method. It is very easy to distinguish Gram-negative bacteria from Gram-positive bacteria and fungus.

Detection of LPS in Practical Samples. To demonstrate the applicability of this new platform to practical sample analysis, quantitative analysis of LPS is performed on different kinds of samples such as injectables, oral solution, tap water, and serum samples of sepsis model mouse during different stages. To compare and correlate with LAL test, we detected the LPS contents of actual samples by LAL assay. As shown in Table 2, LPS was not detected in NaCl injection, glucose injection, water for injection, and calcium gluconate oral solution. Our results are consistent with that of LAL test. Accuracy of this method and the potential matrix effects were explored by analyzing spiked samples. The recovery values of LAL and our method for serum sample of healthy mouse are 117−123% and 80−88%, respectively. The lower recovery of serum sample could be due to the complicated matrix that can exhibit considerable interference. Analyte-independent interference can cause signals in the absence of analyte or inhibits the assay reagents directly. Interference can lead to both artificially increased or decreased results. Matrix interference (nonspecificity) often leads to under-recovery of the spiked amount.[36] In this study, the serum was diluted by 100 times to decrease the interference of sample matrix. The recovery values of our method are between 80 and 114%, which are within an acceptable range.[37] Figure 8 indicates a good correlation ($R^2 = 0.993$) between the two methods.

CONCLUSION

In summary, an easy-to-use, sensitive, specific, and lot-to-lot consistent LPS detection method based on CI-ES in a microfluidic chip coupling rGO with FAM-aptamer is developed. This method only consumes a small amount of sample (the minimum serum volume is 1 μL) for detection, and it does not depend on animal sources, such as horseshoe crabs, hence, redeeming diminishing horseshoe crabs from extinction. Our assay in a lab-on-chip device can detect 7.9 fM (7.9×10^{-4} EU/mL) and 8.3 fM (8.3×10^{-4} EU/mL) for water sample and serum sample, respectively, and the results are well correlated with the gold-standard LAL assay. Moreover, the approach can also make a distinction between Gram-negative and Gram-positive bacteria and fungus. The high specificity and sensitivity make this method truly universal for the determination of other clinical biomolecules by choosing the corresponding aptamer sequences.

ASSOCIATED CONTENT

Supporting Information

The Supporting Information is available free of charge on the ACS Publications website at DOI: 10.1021/acs.analchem.8b05106.

Characterization of GO and rGO, some other conditions optimization, and the degree of interference for competing molecules (PDF)

AUTHOR INFORMATION

Corresponding Authors

*E-mail: jyhan@mit.edu (J.H.).
*E-mail: lhliu02@126.com (L.L.).

ORCID

Wei Ouyang: 0000-0003-4279-661X
Shuwen Liu: 0000-0001-6346-5006
Lihong Liu: 0000-0003-3631-2148

Author Contributions

The manuscript was written through contributions of all authors. All authors have given approval to the final version of the manuscript.

Notes

The authors declare no competing financial interest.

ACKNOWLEDGMENTS

The study was supported financially by the Natural Science Foundation of China (81470161) and the Science and Technology Program of Guangdong Province (2016A040403052), and the Southern Medical University (YD2017N002).

REFERENCES

(1) Cuschieri, J.; Billigren, J.; Maier, R. V. J. *J. Leukocyte Biol.* **2006**, *80*, 1289−1297.
(2) Niehaus, I. *Nigerian Health J.* **2010**, *10*, 26−33.
(3) Lim, S. K.; Chen, P.; Moochhala, S.; Liedberg, B. *Asian Pac. J. Trop. Dis.* **2014**, *4*, 223−223.
(4) Appelmelk, B. J.; van Die, I.; van Vliet, S. J.; Vandenbroucke-Grauls, C. M. J. E.; Geijtenbeek, T. B. H.; van Kooyk, Y. *J. Immunol.* **2003**, *170*, 1635−1639.
(5) < 85> Bacterial endotoxins test. *United States Pharmacopeia 30/National Formulary 25*; The United States Pharmacopeial Convention, Inc., 2007, .
(6) Mészáros, K.; Aberle, S.; Dedrick, R.; Machovich, R.; Horwitz, A.; Birr, C.; Theofan, G.; Parent, J. B. *Blood* **1994**, *83*, 2516−2525.
(7) Bates, D. W.; Parsonnet, J.; Ketchum, P. A.; Miller, E. B.; Novitsky, T. J.; Sands, K.; Hibberd, P. L.; Graman, P. S.; Lanken, P. N.; Schwartz, J. S.; Kahn, K.; Snydman, D. R.; Moore, R.; Black, E.; Platt, R. *Clin. Infect. Dis.* **1998**, *27*, 582−591.
(8) Hardy, E.; Rodriguez, C.; Trujillo, L. E. *Biol. Med.* **2016**, *8*, 277.

DOI: 10.1021/acs.analchem.8b05106
Anal. Chem. 2019, 91, 2360−2367

(9) Rydosz, A.; Brzozowska, E.; Górska, S.; Wincza, K.; Gamian, A.; Gruszczynski, S. *Biosens. Bioelectron.* **2016**, *75*, 328−336.
(10) Kalita, P.; Dasgupta, A.; Sritharan, V.; Gupta, S. *Anal. Chem.* **2015**, *87*, 11007−11012.
(11) Bruno, J. G.; Carrillo, M. P.; Phillips, T. *Folia Microbiol.* **2008**, *53*, 295−302.
(12) Jiang, G.; Wang, J.; Yang, Y.; Zhang, G.; Liu, Y.; Lin, H.; Zhang, G.; Li, Y.; Fan, X. *Biosens. Bioelectron.* **2016**, *85*, 62−67.
(13) Hu, J.; Easley, C. J. *Analyst* **2011**, *136*, 3461−3468.
(14) Kim, S. E.; Su, W.; Cho, M.; Lee, Y.; Choe, W. S. *Anal. Biochem.* **2012**, *424*, 12−20.
(15) Su, W.; Lin, M.; Lee, H.; Cho, M.; Choe, W. S.; Lee, Y. *Biosens. Bioelectron.* **2012**, *32*, 32−36.
(16) Yang, Q. H.; Lu, W.; Yang, Y. G.; Wang, M. Z. *Carbon* **2008**, *46*, 1−1.
(17) Zhou, T.; Yu, H.; Liu, M.; Yang, Y. *Chin. J. Chem.* **2015**, *33*, 125−130.
(18) Zhang, Z.; Yang, J.; Pang, W.; Yan, G. *RSC Adv.* **2017**, *7*, 54920−54926.
(19) Duch, M. C.; Budinger, G. R. S.; Liang, Y. T.; Soberanes, S.; Urich, D.; Chiarella, S. E.; Campochiaro, L. A.; Gonzalez, A.; Chandel, N. S.; Hersam, M. C.; Mutlu, G. M. *Nano Lett.* **2011**, *11*, 5201−5207.
(20) Ko, S. H.; Song, Y. A.; Kim, S. J.; Kim, M.; Han, J.; Kang, K. H. *Lab Chip* **2012**, *12*, 4472−4482.
(21) Cheow, L. F.; Han, J. Y. *Anal. Chem.* **2011**, *83*, 7086−7093.
(22) Lan, M.; Wu, J.; Liu, W.; Zhang, W.; Ge, J.; Zhang, H.; Sun, J.; Zhao, W.; Wang, P. *J. Am. Chem. Soc.* **2012**, *134*, 6685−6694.
(23) Voss, S.; Fischer, R.; Jung, G.; Wiesmüller, K. H.; Brock, R. *J. Am. Chem. Soc.* **2007**, *129*, 554−561.
(24) Wang, Y. H.; Deng, H. H.; Liu, Y. H.; Shi, X. Q.; Liu, A. L.; Peng, H. P.; Hong, G. L.; Chen, W. *Biosens. Bioelectron.* **2016**, *80*, 140−145.
(25) Zhou, Y.; Bao, Q.; Tang, L.; Zhong, Y.; Loh, K. P. *Chem. Mater.* **2009**, *21*, 2950−2956.
(26) Leon, L. R. *Front. Biosci., Landmark Ed.* **2004**, *9*, 1877−1888.
(27) Gao, L. T.; Seliskar, C. J. *Chem. Mater.* **1998**, *10*, 2481−2489.
(28) Kim, S. J.; Song, Y.; Han, J. *Chem. Soc. Rev.* **2010**, *39*, 912−922.
(29) Ouyang, W.; Ye, X.; Li, Z.; Han, J. *Nanoscale* **2018**, *10*, 15187−15194.
(30) Gong, L.; Ouyang, W.; Li, Z.; Han, J. *AIP Adv.* **2017**, *7*, No. 125020.
(31) Ruff, K. M.; Snyder, T. M.; Liu, D. R. *J. Am. Chem. Soc.* **2010**, *132*, 9453−9464.
(32) Shihabi, Z. K. *Electrophoresis* **2002**, *23*, 1612−1617.
(33) Lagarrigue, M.; Bossée, A.; Bégos, A.; Delaunay, N.; Varenne, A.; Gareil, P.; Bellier, B. *Journal of Chromatography A* **2008**, *1178*, 239−247.
(34) Gao, H.; Yang, S.; Han, J.; Xiong, J.; Kong, W.; Li, C.; Liao, G.; Fu, Z. *Chem. Commun.* **2015**, *51*, 12497−12500.
(35) Wacker, C.; Prkno, A.; Brunkhorst, F. M.; Schlattmann, P. *Lancet Infect. Dis.* **2013**, *13*, 426−435.
(36) Schwickart, M.; Vainshtein, I.; Lee, R.; Schneider, A.; Liang, M. *Bioanalysis* **2014**, *6*, 1939−1951.
(37) *Standard Methods for the Analysis of Water and Wastewater*, 18th ed.; American Public Health Association: Washington, DC, 1992.

DOI: 10.1021/acs.analchem.8b05106
Anal. Chem. 2019, 91, 2360−2367